

Hydrated subducted crust at 100–250 km depth

Geoffrey A. Abers*

Geology Department, University of Kansas, Lawrence, KS 66044, USA

Received 31 August 1999; received in revised form 10 January 2000; accepted 11 January 2000

Abstract

Seismic waves that travel along the surface of subducted slabs provide a means to infer petrology to considerable depth. At high frequencies (0.5–10 Hz) they are particularly sensitive to the presence and state of subducted oceanic crust. New observations reveal systematic distortion of body waves in all north Pacific subduction zones, when signals traverse slabs at 100–250 km depths, suggesting that crust remains distinct to these depths. The signals show waveguide behavior at the scale of a few kilometers: short-wavelength, high-frequency energy (≥ 3 Hz) is delayed 5–7% relative to that of low frequencies (≥ 1 Hz), systematically at all subduction zones. To explain these observations, velocities in a low-velocity layer 1–7 km thick, likely subducted crust, must remain seismically slow relative to surrounding mantle at these depths. Hence, it seems unlikely that subducted crust has completely converted to eclogite, as often assumed. Inferred velocities within subducted crust are similar to those estimated for blueschists, suggesting that hydrous assemblages persist past the volcanic front. © 2000 Elsevier Science B.V. All rights reserved.

Keywords: subduction; oceanic crust; wave dispersion; metamorphism; velocity structure

1. Introduction

As it subducts, oceanic crust dewateres and densifies. A dry basaltic crust undergoes a series of reactions to generate high-density eclogite, triggered by phase changes that begin at 20–50 km depth [1,2]. However, the basalt-to-eclogite reaction sequence may be kinetically hindered, so basalt might persist metastably [3,4]. Moreover, wet crust should form hydrous blueschist-facies minerals that may persist to great depths at low temperatures [2,5] and perhaps transport water into the deep mantle. Such slab dehydration and den-

sification could play a key role in the mantle volatile budget, in the generation of earthquakes, and in driving subducting slabs. These possibilities suggest a seismological test: seismic velocities in eclogite are nominally faster than surrounding mantle at upper mantle conditions, while basalt is 10–20% slower and less dense than peridotite [6,7] and lawsonite blueschist has velocities and densities $\sim 5\%$ slower [8,9]. Previous seismic measurements show differing structures at individual arcs, showing fast velocities at the top of the Tonga slab [10], compared to slow velocities atop Japan [6,11] and Alaska [12], leaving the basic observations ambiguous.

Here, we investigate several subducting plates at 100–250 km depths, by studying the effect of seismic wave propagation along the slab surface on body wave pulse shapes. At wavelengths of a

* Present address: Department of Earth Sciences, Boston University, Boston, MA 02215, USA. Tel.: +1-617-353-2532; Fax: +1-617-353-3290; E-mail: abers@bu.edu

few kilometers the distortions to body waves are dispersive, and high-frequency arrival times often differ from low-frequency ones [7,10,12]. This is precisely the scale over which subducted crust should have an effect on wave behavior. For energy traveling long distances along the surface of the slab, the effect can then be treated as dispersion caused by a waveguide – subducted crust is a contiguous layer surrounded on each side by mantle.

2. Seismic dispersion

We measure body wave dispersion for five subduction zones in the north Pacific, for events 100–250 km deep. At each subduction zone, recently deployed Global Seismic Network stations provide excellent samples of regional broadband waveforms for events between 1993 and 1997. Raypaths vary from 100 km to 1000 km in length, although most dispersion measurements are for paths 200–600 km long (Fig. 1). These measurements provide information on the variation in seismic velocity within the slab as a function of frequency, which ultimately constrains the layered structure of the top of the slab.

Dispersion is analyzed between 0.25 and 7.5 Hz, the frequencies at which energy is largest in these signals (Fig. 2). The measurements extract the time of the maximum energy in an arrival as a function of frequency, and essentially provide group arrival times. These times are measured relative to a fiducial low-frequency measurement, here at 0.5 Hz (the lowest frequency to give consistently stable measurements), and so provide a measure of travel time relative to the low-frequency arrival; absolute travel times are subject to considerable uncertainty due to mislocation and path effects so have less utility. The differential group lag times increase systematically with path length within the slab and are negligible for paths that do not traverse the slab [12], suggesting that slab structure is responsible.

Suites of dispersion measurements are stacked to give a group velocity curve for each arc and phase (Fig. 3). To convert differential group lags to group velocity variations, we estimate the por-

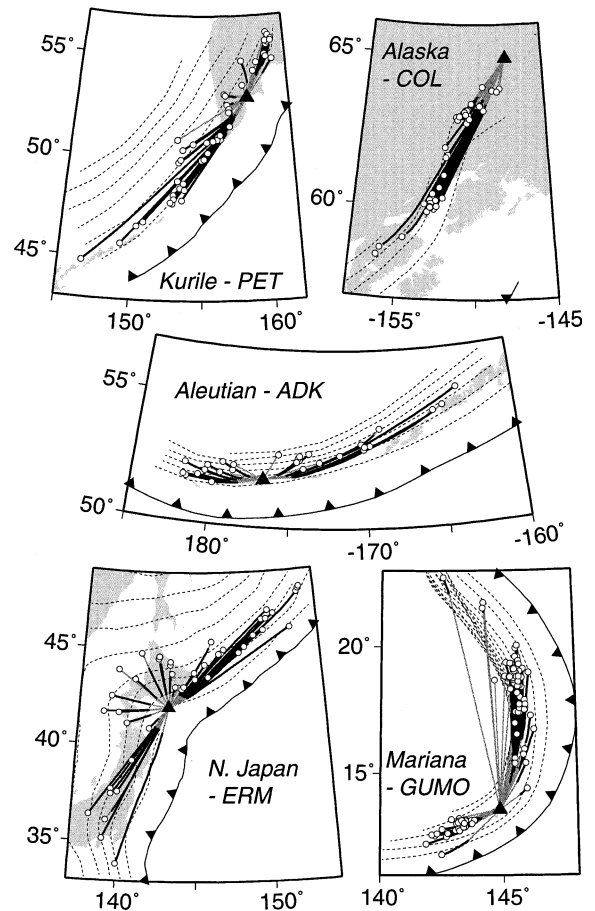


Fig. 1. Subducting slabs and raypaths, stations (triangles), and earthquakes (circles); arc and station code labeled. Rays are traced from station to event via a fast Eikonal-equation solver [29,30] through a three-dimensional slab model. In these models, the slab is uniformly 5% faster than surrounding mantle and is 75 km thick. The top surface follows seismicity from teleseismic relocations [31] and local catalogs in Alaska and Japan. Tests show group velocity estimates vary less than 0.2% for slab velocity anomalies ranging 4–10% and slab locations shifting ± 20 km. Seismicity is contoured (dashes) at 50 km intervals, 100 km for Kuriles (all depths) and Japan (depths > 200 km). Raypaths are divided into two segments, outside the slab (gray lines) and inside (thick black lines); the latter are used in group velocity calculations.

tion of each raypath within a three-dimensional model of slab thermal structure (Fig. 1), an estimate of the path length for the long-period signals. Most raypaths are near horizontal in slabs, and the ray bottoming depths never lie more than

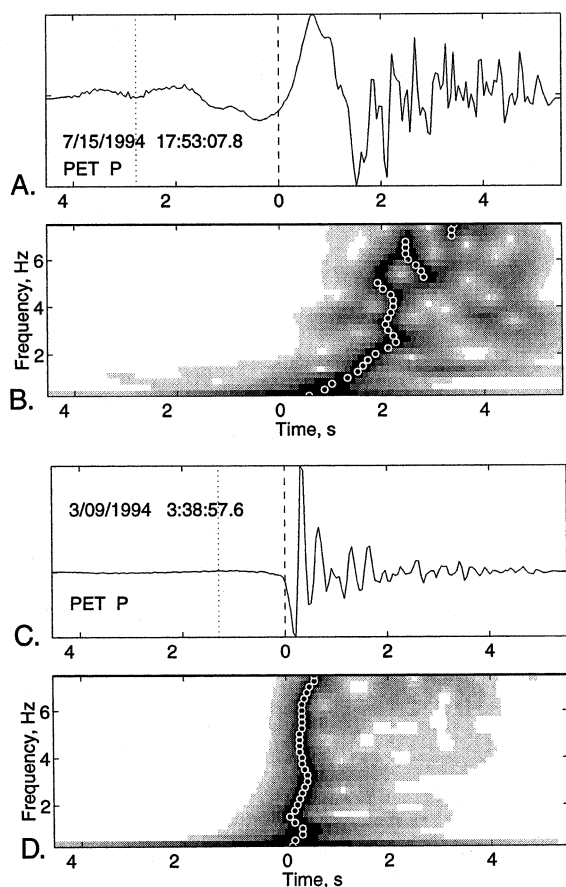


Fig. 2. Examples of a dispersed and non-dispersed P-wave train. (A) Dispersed P-wave, vertical component, recorded at station PET from an event 5.29° distant at 118 km depth, with predicted (dotted) and observed (dashed) travel times. Low frequencies arrive 1.5–2 s ahead of high frequencies. Note that predictions are from global travel-time tables so can show random misfits of several seconds due to mislocation and path effects. (B) Dispersion measurement. Seismogram is filtered by a series of narrow-band filters [32] with central frequencies ranging from 0.25 to 7.5 Hz, following deconvolution to displacement. At each frequency, the instantaneous amplitude envelope is calculated and normalized to its peak value. Envelopes are contoured together, and peaks are automatically picked for each frequency (white circles). Picked lag times are subtracted from that of a low-frequency standard, here 0.5 Hz, to remove effects of mislocated hypocenters and erroneous velocities. (C) Non-dispersed P-wave recorded at PET, from an event 1.06° distant and 189 km deep; signals from this event do not sample the slab. (D) Dispersion measurement on non-dispersed P-wave.

50 km deeper than the earthquake source. Hence, the signals sample slabs at depths comparable to the range in source depths, 100–250 km.

These dispersion measurements show that high-frequency signals are delayed relative to low frequencies, in all five arcs. High-frequency delays relative to 0.5 Hz are typically near 4–7% (Fig. 3), and the 0.5 Hz arrival shows additional 1–2% delay relative to 0 Hz. S-waves generally show similar delays as P-waves. Four arcs show indistinguishable dispersion curves and all P-waves show similar dispersion. The Mariana–GUMO observations show significantly greater S-wave dispersion, but there is very little energy in these

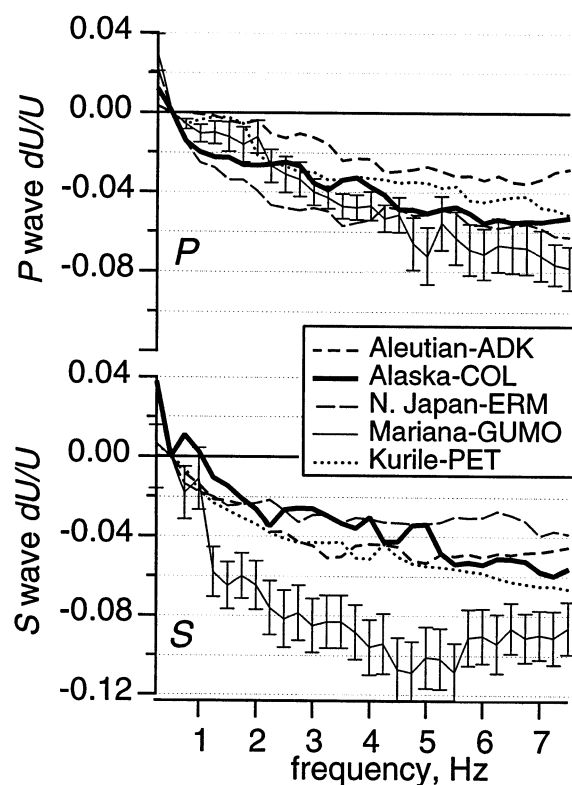


Fig. 3. Group velocity variations with frequency for five arcs, for P- and S-waves. dU/U is fractional variation in group velocity relative to 0.5 Hz. Curves are ensemble averages based on lag measurements (e.g. Fig. 2) and slab path lengths (Fig. 1), including only those paths spending at least 5 s within the slab; Table 1 gives numbers of records averaged. Error bars in average group velocity, 2σ uncertainties in mean, are shown only for GUMO (Guam), which consistently had larger uncertainties than others.

S-waves above 4 Hz and high arc curvature near GUMO lends greater uncertainty to raypath estimates. Overall, delayed high-frequency arrivals of 5–8% are typical of the best-constrained paths.

3. Crustal waveguide

The simplest structure to produce such dispersion is a planar low-velocity layer (LVL) in an otherwise homogeneous medium, such as slow subducted crust surrounded by faster mantle rocks. A LVL would act as a waveguide, trapping high-frequency energy but not affecting low-frequency energy; high-frequency energy would travel at the speed of the channel while low-frequency energy would not.

In order to constrain the LVL properties, fundamental-mode acoustic dispersion curves are fit to the observed dispersion via least-squares minimization (Table 1). The shape of the dispersion curves depends only upon LVL thickness and velocity contrasts between LVL and surrounding medium, and can be estimated analytically [10]. These fits show estimates of LVL thickness in the range 1–7 km and velocities consistently 5–7% lower than background for four of the five arcs (nearly 10% for the problematic Mariana data). All slabs show dispersed wave trains for

along-strike propagation, in a manner suggesting a LVL atop all five slabs. The amplitude of the dispersion is very similar between all arcs, and both P- and S-waves indicate similar velocities.

Hence, a 5–7% slow layer is common to the top of subducting slabs at depths of 100–250 km. Although the LVL thickness may be biased to low values, it is generally similar to or rather less than the 7 km thickness of subducting crust; in particular, H is greater than the 100–500 m thickness of subducted sediment inferred for these arcs [13]. We conclude that subducted crust, or a parallel nearby layer of comparable thickness, persists as a LVL to considerable depth in most subduction zones.

The one known exception is the reported pattern for Tonga, where high frequencies precede low-frequency arrivals at stations in New Zealand [7,10,14]. The Tonga paths are generally much longer than those described above and many sources are much deeper, so that nearly all raypaths bottom at or below 400 km. Because different depths are being sampled beneath Tonga, it is possible that the high-velocity layer behavior inferred there describes the state of slabs at depths below 250 km depth and may reflect eventual eclogite formation.

There is no evidence for strong path dependence that would be expected if the LVL were a

Table 1
Estimated waveguide velocities and dimensions

Arc	Station	Phase	Events	V/V_0	H (km)	r.m.s. misfit
Mariana	GUMO	P	20	0.925 ± 0.038	1.1 ± 1.0	0.0036
		S	26	0.897 ± 0.034	2.3 ± 0.9	0.0083
N. Japan	ERM	P	25	0.940 ± 0.022	3.7 ± 0.9	0.0044
		S	18	0.965 ± 0.018	5.4 ± 2.0	0.0029
Kurile-Kamchatka	PET	P	19	0.956 ± 0.013	1.9 ± 1.0	0.0040
		S	23	0.947 ± 0.032	3.1 ± 1.6	0.0027
Aleutian	ADK	P	16	0.964 ± 0.011	1.6 ± 1.0	0.0025
		S	14	0.949 ± 0.022	2.9 ± 1.6	0.0032
Alaska	COL	P	29	0.950 ± 0.015	2.3 ± 1.1	0.0064
		S	24	0.951 ± 0.169	2.0 ± 2.0	0.0062

V/V_0 is the velocity within the LVL normalized to that of surrounding medium, and H is LVL thickness. These are estimated from fits to group velocity dispersion curves (Fig. 3) assuming a fundamental-mode response for a simple acoustic waveguide [10]. R.m.s. misfit is in units of dU/U , and uncertainties are 95% bootstrap confidence limits. Thickness estimates are calculated for nominal $V_0 = 8.5$ km/s (P-wave). Sensitivity tests, from inversions of theoretical elastic full-waveform seismograms [19], show that V/V_0 should be recoverable to within 1%. However, H may be underestimated by up to 50% because high-frequency higher-mode energy cannot be accounted for in the fits, since the precise positions of sources relative to the LVL are poorly known.

consequence of anisotropy. The signals analyzed here sample predominantly along strike paths, yet very similar 5–8% slow velocities have been obtained from up-dip measurements beneath the east Aleutians [15] and Japan [11]. The similarity of P- and S-wave velocity perturbations also suggest the LVL is approximately isotropic with a Poisson ratio similar to that of the surrounding mantle.

The existence of a 5–7% LVL atop slabs has been previously inferred from other methods sampling different ray geometries, notably converted wave studies, mostly from Japan [7,9,11,16] but also the Aleutians [15]. This abundance of such observations, of both P- and S-waves, along-strike, up-dip paths and mode conversions, suggests that the LVL is a robust feature common to most subduction zones.

4. Waveguide structure

In order to efficiently trap energy, as observed here, the LVL must exhibit several properties. Although a full exploration of waveguide phenomena is beyond the scope of this paper, recent studies synthesizing guided waves in fault zones (e.g. [17,18]) provide several relevant constraints. First, these finite-difference simulations show that waveguides are effectively excited only when sources are within 1–2 times the LVL thickness from its center. Thus, the waveguide phenomenon seen here is generated by earthquakes within a few kilometers of (or within) the LVL, as observed in Japan [11]. Second, although gradual bends or changes in LVL geometry do not significantly affect dispersion, large jogs or heterogeneities within the LVL can completely disrupt trapped wave propagation if their dimension exceeds the waveguide width. Third, details of source location or attenuation can affect spectral content in ways that add uncertainty to layer thickness. Independent sensitivity tests utilizing full-waveform synthesis [19], not shown, suggest that LVL thickness is underestimated when higher-mode excitation is not taken into account by as much as 50% (Table 1). Finally, preliminary calculations suggest that the waveguide can only trap high-frequency en-

ergy if the boundary is sharp relative to the dominant wavelength of trapped energy; i.e. the boundary must grade from high to low velocities over a distance small compared to the LVL thickness. Phenomena that produce gradual boundaries, such as temperature variations, are unlikely to produce the requisite LVL. These constraints are all consistent with the LVL being equated to subducted crust.

5. Constraints on composition

The relative velocity estimates made here are compared to a variety of rock assemblages suspected to be present at depth, by comparing their velocities at nominally comparable conditions (4 GPa, 650°C) to that of a typical peridotite assemblage (Fig. 4). At pressures above 1 GPa dry gabbro should be stable as eclogite, and should exhibit velocities 1–3% faster than typical mantle peridotite at slab conditions [6,7,9]. Instead, north Pacific waveguides are slow rather than fast ($V/V_0 < 1$), ruling out the possibility of a fully eclogitized layer. Alternatively, if dry basalt or gabbroic crust persists metastably to depth, then it would be 10–13% slower than harzburgite. A 5–10 km thick, ~15% slow LVL has been observed beneath southern Japan but only to 50–60 km depth [20], suggesting that gabbro may persist to moderate depths, at least in this unusually young and hot subduction zone. However, the 5–7% slow LVL observed here is faster than gabbro, so metastable gabbro does not obviously persist deeper. (Note that gabbro compresses more easily than peridotite, so velocity differences diminish with increasing depth.) A mixture of gabbro and eclogite is possible, perhaps from incomplete eclogitization, but the observations made here would require similar proportions of the two end members to be present in all arcs observed.

A dewatering slab might hydrate the overlying mantle wedge to produce a serpentinized layer that parallels the subducting slab [21]. Serpentine has an exceedingly high Poisson ratio, ~0.37 (extrapolating to 4 GPa from [22,23], following [24]), so S-waves are affected by serpentinization more than P. Velocities in partly serpentinized rocks lie

close to some but not all of the observed LVL values, for 0.5–1.0 wt% H₂O, corresponding to rocks with 5–10% serpentine (Fig. 4); these compositions give Poisson ratios at the high side of the observed uncertainties. More problematic, as discussed above the waveguide excitation would require a continuous serpentinized zone following the slab with sharp yet fairly smooth boundaries and a thickness of a few kilometers (the top of subducted crust could be the lower such boundary). Given the likely variability in serpentinization in real mantle rock such a sharp serpentinite

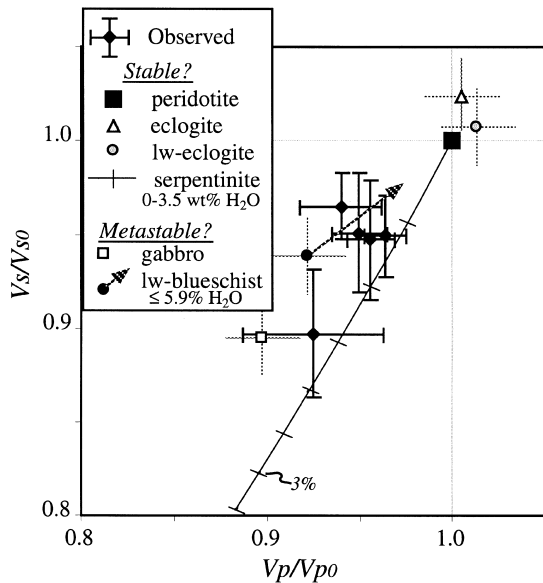


Fig. 4. Comparison of observed to predicted seismic velocities. Observed velocities are that of the waveguide relative to surrounding media (mantle peridotite), with 95% confidence limits, from Table 1. Rock velocities are calculated for several theoretical rocks at 4 GPa and 650°C, the approximate conditions sampled, from single-mineral elastodynamic properties following [9,24]. Velocities are normalized to that of pyrolite to remove first-order variations with temperature and pressure. Uncertainties for rocks assumed to be 0.02%, reflecting uncertainties in averaging and compositional variability. Compositions for lawsonite (lw) blueschist and eclogite from [28], mantle peridotite (pyrolite-II) and gabbro from [1,6], and lw-eclogite derived from [2]. Serpentinite calculated by adding water to the peridotite, substituting increasing amounts of antigorite for forsterite and enstatite following [33], and elastic parameters of [22,23]. The lw-blueschist composition is calculated in a fully hydrated system [28] and would underestimate velocities in partly hydrated crust, as indicated by arrow.

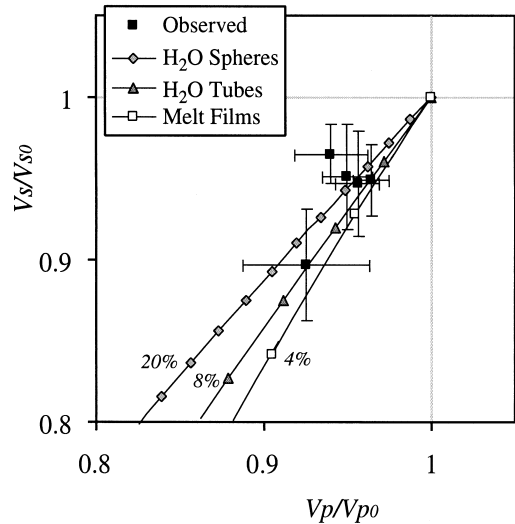


Fig. 5. Effect of fluids on seismic velocities, and comparison to observations. Observed velocities as Fig. 4. Effect of water calculated for isolated spherical pores following [34] or narrow, interconnected tubules following [35]; isolated pores are found in hydrostatic experiments in pyroxenite [25] although dihedral angles may decrease to form interconnected tubules at high pressures [26]. Effect of melt is calculated for penny-shaped cracks [36] with aspect ratio of 0.05, as appears common for low-degree melts in ultramafic rocks [27]. Reference rock is pyrolite-II as Fig. 4; elastic properties for melt from [37] and water from equation of state calibrated by [38]; rock-water properties calculated at 650°C and 4 GPa while rock-melt properties calculated at 850°C and 4 GPa. Symbols denote fluid content increments of 2% by volume. Note high fluid contents required for a hypothetical water layer.

layer seems unlikely, although cannot be ruled out on the basis of seismic velocities alone.

Free fluids (H₂O or melt) may reduce seismic velocities (Fig. 5). Experiments suggest that water at slab conditions should form in isolated pores [25], but porosities of 5–10% would be required to explain the observed LVL velocities (Fig. 5, spheres) over the entire LVL width. This would require far more water than available during subduction [2]. Even were water to lie in interconnected, needle-like tubes, as may be possible at pressures > 3 GPa [26], 2–4% porosity would be required in situ; it is unclear how that much water could be retained without escaping. Hence, it seems unlikely that the low velocities are generated by the presence of free water.

As well, a partial-melt layer atop the subducted

slab is problematic. At hydrostatic conditions melt may be well approximated by penny-shaped cracks [27], at 1–2% porosity to explain the observed velocities (Fig. 5, films). For such melt configurations, the observed ratios of S- to P-wave velocities lie above that predicted by the melt calculation, in some cases beyond the 95% uncertainties. As well, a several kilometers thick partly molten layer is difficult to reconcile with thermal models that suggest subsolidus conditions at the top of the slab [28], and perhaps with the observation that earthquakes nucleate within a few kilometers of the LVL as high temperatures are rarely associated with brittle failure.

6. Summary

At pressures above 1 GPa and typical slab temperatures, hydrated gabbros should form blueschists and hold several wt% water [28]. Lawsonite (lw) blueschists have velocities similar to the LVL observed here [9], 5–8% slower than peridotite, and hence form a reasonable candidate for the LVL (the small discrepancy in Fig. 4 can be attributed to the model blueschist being fully water-saturated [28]). However, the low velocities require the presence of amphiboles and chlorite, both of which likely break down at depths greater than 65–100 km. In cold slabs, blueschists might persist metastably to greater depths, at least in the coarse-grained gabbroic layer [8]; such a scenario could explain our observations well. Some hydrous phases, notably lawsonite, may persist to exceedingly high pressures in sufficiently cold slabs [5]. However, the reported assemblages (e.g. 'lw-eclogite' on Fig. 4) have seismic velocities that are insignificantly different (–1 to +2%) from mantle peridotites, because seismic velocities of lawsonite are comparable to those of anhydrous minerals. Without significant quantities of amphibole, chlorite, or other slow minerals, seismic velocities in subducted crust cannot obviously lie 5–8% below those of mantle peridotite, as observed, at least given the current knowledge of elasticity in hydrous minerals.

In summary, it is difficult to match velocities in the LVL with eclogite at the 100–250 km depths

required. The best candidate composition seems to be metastable blueschist, in a layer that comprises 25–80% of the 7 km thick subducted crust. Other possibilities include partial eclogitization, substantial free fluid, or a sharply bound serpentinite layer. In any case, the low-velocity layer is a persistent feature of many subduction zones, an observation that suggests a significant volatile fraction may survive dewatering and remain in the slab past the volcanic front.

Acknowledgements

GSN seismograms provided by the IRIS Data Management Center. J. Hole and R. Herrmann provided travel time and waveform modeling programs. Although other methods were used A. Levshin provided advice in dispersion analysis. Interpretations benefited from discussions with and reviews by B. Hacker, G. Helffrich, S. Peacock, and T. Plank, and an anonymous reviewer. Supported by National Science Foundation Grant EAR-9725601. *[RV]*

References

- [1] A.E. Ringwood, D.H. Green, An experimental investigation of the gabbro-eclogite transformation and some geophysical implications, *Tectonophysics* 3 (1966) 383–427.
- [2] M.W. Schmidt, S. Poli, Experimentally based water budgets for dehydrating slabs and consequences for arc magma generation, *Earth Planet. Sci. Lett.* 163 (1998) 361–379.
- [3] T.J. Ahrens, G. Schubert, Gabbro-eclogite reaction rate and its geophysical significance, *Rev. Geophys. Space Phys.* 13 (1975) 383–400.
- [4] S.H. Kirby, E.R. Engdahl, R. Denlinger, Intraslab earthquakes and arc volcanism: dual physical expressions of crustal and uppermost mantle metamorphism in subducting slabs, in: G.E. Bebout, D. Scholl, S. Kirby (Eds.), *Subduction: Top to Bottom*, *Geophys. Monogr.* 96 (1996) 195–214, AGU, Washington, DC.
- [5] A.R. Pawley, J.R. Holloway, Water sources for subduction zone volcanism: new experimental constraints, *Science* 260 (1993) 664–667.
- [6] G.R. Helffrich, S. Stein, Study of the structure of the slab-mantle interface using reflected and converted seismic waves, *Geophys. J. Int.* 115 (1993) 14–40.
- [7] D. Gubbins, A. Barnicoat, J. Cann, Seismological con-

- straints on the gabbro–eclogite transition in subducted oceanic crust, *Earth Planet. Sci. Lett.* 122 (1994) 89–101.
- [8] B.R. Hacker, Eclogite formation and the rheology, buoyancy, seismicity, and H₂O content of oceanic crust, in: G.E. Bebout, D. Scholl, S. Kirby (Eds.), *Subduction: Top to Bottom*, *Geophys. Monogr.* 96 (1996) 337–346, AGU, Washington, DC.
- [9] G. Helffrich, Subducted lithospheric slab velocity structure: Observations and mineralogical inferences, in: G.E. Bebout, D. Scholl, S. Kirby (Eds.), *Subduction: Top to Bottom*, *Geophys. Monogr.* 96 (1996) 215–222, AGU, Washington, DC.
- [10] D. Gubbins, R. Snieder, Dispersion of P waves in subducted lithosphere: Evidence for an eclogite layer, *J. Geophys. Res.* 96 (1991) 6321–6333.
- [11] T. Matsuzawa, N. Umino, A. Hasegawa, A. Takagi, Upper mantle velocity structure estimated from PS-converted wave beneath the north-eastern Japan Arc, *Geophys. J. R. Astron. Soc.* 86 (1986) 767–787.
- [12] G.A. Abers, G. Sarker, Dispersion of regional body waves at 100–150 km depth beneath Alaska: In situ constraints on metamorphism of subducted crust, *Geophys. Res. Lett.* 23 (1996) 1171–1174.
- [13] T. Plank, C.H. Langmuir, The chemical composition of subducting sediment and its consequences for the crust and mantle, *Chem. Geol.* 145 (1998) 325–394.
- [14] R.D. van der Hilst, R. Snieder, High-frequency precursors to P wave arrivals in New Zealand: Implications for slab structure, *J. Geophys. Res.* 101 (1996) 8473–8488.
- [15] G. Helffrich, G.A. Abers, Slab low-velocity layer in the eastern Aleutian subduction zone, *Geophys. J. Int.* 130 (1997) 640–648.
- [16] T. Iidaka, M. Mizoue, P-wave velocity structure inside the subducting Pacific plate beneath the Japan region, *Phys. Earth Planet. Interact.* 66 (1991) 203–213.
- [17] Y.-G. Li, J.E. Vidale, Low-velocity fault-zone guided waves: numerical investigations of trapping efficiency, *Bull. Seismol. Soc. Am.* 86 (1996) 371–378.
- [18] H. Igel, Y. Ben-Zion, P.C. Leary, Simulation of SH- and P-SV-wave propagation in fault zones, *Geophys. J. Int.* 128 (1997) 533–546.
- [19] C.Y. Wang, R.B. Herrmann, A numerical study of P-, SV-, and SH-wave generation in a plane layered medium, *Bull. Seismol. Soc. Am.* 70 (1980) 1015–1036.
- [20] S. Hori, H. Inoue, Y. Fukao, M. Ukawa, Seismic detection of the untransformed ‘basaltic’ oceanic crust subducting into the mantle, *Geophys. J. R. Astron. Soc.* 83 (1985) 169–197.
- [21] C. Meade, R. Jeanloz, Deep-focus earthquakes and recycling of water into the Earth’s mantle, *Science* 252 (1991) 68–72.
- [22] N.I. Christensen, Poisson’s ratio and crustal seismology, *J. Geophys. Res.* 101 (1996) 3139–3156.
- [23] J.A. Tyburczy, T.S. Duffy, T.J. Ahrens, M.A. Lange, Shock wave equation of state of serpentine to 150 GPA: Implications for the occurrence of water in the Earth’s lower mantle, *J. Geophys. Res.* 96 (1991) 18011–18028.
- [24] C.R. Bina, G.R. Helffrich, Calculation of elastic properties from thermodynamic equation of state principles, *Annu. Rev. Earth Planet. Sci.* 20 (1992) 527–552.
- [25] E.B. Watson, A. Lupulescu, Aqueous fluid connectivity and chemical transport in clinopyroxene-rich rocks, *Earth Planet. Sci. Lett.* 117 (1993) 279–294.
- [26] K. Mibe, T. Fujii, A. Yasuda, Control of the location of the volcanic front in island arcs by aqueous fluid connectivity in the mantle wedge, *Nature* 401 (1999) 259–262.
- [27] U.H. Faul, D.R. Toomey, H.S. Waff, Intergranular basaltic melt is distributed in thin, elongated inclusions, *Geophys. Res. Lett.* 21 (1994) 29–32.
- [28] S.M. Peacock, The importance of blueschist → eclogite dehydration in subducting oceanic crust, *Geol. Soc. Am. Bull.* 105 (1993) 684–694.
- [29] J.E. Vidale, Finite-difference calculation of travel times in three dimensions, *Geophysics* 55 (1990) 521–526.
- [30] J.A. Hole, B.C. Zelt, 3-D finite-difference reflection travel times, *Geophys. J. Int.* 121 (1995) 427–434.
- [31] E.R. Engdahl, R. van der Hilst, R. Buland, Global teleseismic earthquake relocation with improved travel times and procedures for depth determination, *Bull. Seismol. Soc. Am.* 88 (1998) 722–743.
- [32] A. Dziewonski, S. Bloch, M. Landisman, A technique for the analysis of transient seismic signals, *Bull. Seismol. Soc. Am.* 59 (1969) 427–444.
- [33] P. Ulmer, V. Trommsdorff, Serpentine stability to mantle depths and subduction-related magmatism, *Science* 268 (1995) 858–861.
- [34] J.P. Watt, G.F. Davies, R.J. O’Connell, The elastic properties of composite materials, *Rev. Geophys. Space Phys.* 14 (1976) 541–563.
- [35] G.M. Mavko, Velocity and attenuation in partially molten rocks, *J. Geophys. Res.* 85 (1980) 5173–5189.
- [36] H. Schmeling, Numerical models on the influence of partial melt on elastic, anelastic and electric properties of rocks, Part I: elasticity and anelasticity, *Phys. Earth Planet. Interact.* 41 (1985) 34–57.
- [37] H. Sato, I.S. Sacks, T. Murase, C.M. Scarfe, Thermal structure of low velocity zone derived from laboratory and seismic investigations, *Geophys. Res. Lett.* 15 (1988) 1227–1230.
- [38] M.C. Johnson, D. Walker, Brucite [Mg(OH)₂] and the molar volume of H₂O to 15 GPa, *Am. Mineral.* 78 (1993) 271–284.